Magnetic Properties

The Magnetic Möbius Strip: Synthesis, Structure, and Magnetic Studies of Odd-Numbered Antiferromagnetically Coupled Wheels**

Olivier Cador, Dante Gatteschi, Roberta Sessoli, Finn K. Larsen, Jacob Overgaard, Anne-Laure Barra, Simon J. Teat, Grigore A. Timco,* and Richard E. P. Winpenny**

The previously reported cyclic 3d-metal structures, from the first—the ferric wheel of Lippard and co-workers[1]—to the largest all contain an even number of metal centres.[2] There are very few odd-numbered cyclic structures larger than three; all are pentametallic and feature polydentate inflexible ligands.[3] Raptis and co-workers have very recently reported a nine-membered ring but only as part of higher nuclearity structures.[4] It is difficult to rationalize the absence of odd-numbered wheels, especially as odd-numbered metallocrowns, that is, wheels centered with a further metal cation, are known.[5] This is particularly frustrating because the magnetic properties of such wheels should be of great interest to physicists interested in magnetic frustration.[6] Spin frustration is, in turn, important in areas as diverse as high temperature superconductors[7] and CMR materials.[8] Herein we report the first detailed magnetic characterization of an odd-numbered wheel larger than a triangle. The new molecular species synthesized allows us to study frustration at a mesoscopic scale at which quantum calculations are still possible; hopefully the understanding gained here can later be applied more generally to other frustrated systems.

In a preceding paper[9] we have shown how the chemistry of $[Cr_8F_8(O_2CCMe_3)_{16}]$ can be exploited to produce a series of heterometallic analogues $[R_2NH_2][Cr_7MF_8(O_2CCMe_3)_{16}]$, in which M = Ni^{II} **1**, Co^{II}, Mn^{II}, or Fe^{II} and R can be a range of alkyl groups from methyl to *n*-octyl. The secondary ammonium cation is found encapsulated within the metal wheel, and this suggested that if we varied the size of the cation we might be able to vary the size of the wheel.

The reaction of hydrated chromium(III) fluoride with basic nickel carbonate in pivalic acid in the presence of dicyclohexylamine, followed by crystallization from THF/toluene produced well-shaped hexagonal crystals. Elemental analysis and electrospray mass spectroscopy (ESMS) provide convincing evidence for the formation of $[(C_6H_{11})_2NH_2][Cr_8NiF_9(O_2CCMe_3)_{18}]$ **2**. The ESMS spectrum of **2** contains a peak for the anionic wheel in the negative-ion spectrum and two significant peaks in the positive-ion spectrum for the molecular ion plus one sodium as well as for the ring plus two sodium ions. These are the only significant high-mass peaks.

The crystals of **2** appear to be single, but the X-ray diffraction pattern has an extraordinary distribution. Proper Bragg diffraction spots are found within a rather flat spheroidal shaped volume of reciprocal space and with pronounced diffuse scattering in the reciprocal planes perpendicular to the apparent sixfold crystal axis of rotation. This makes it difficult to integrate the Bragg intensities for determining structure factors and thus also creates a problem in assigning the space group. The structure can either be described in some hexagonal space groups or in the orthorhombic *Pbna* space group, which gives the lower internal *R* value of integrated reflections. Solving the structure in *Pbna* reveals a nona-metallic core, bridged by single atoms. Atoms of the nearest-neighbor octahedral coordination sphere can be located but the atomic structure does not develop further by subsequent least-squares refinement and difference Fourier methods. Undoubtedly there is much disorder of the outer parts of the pivalate ligands. The combined information of Bragg intensities and distribution of diffuse scattering supports the following model of the structure: The molecules that have a nine-membered ring form layers, and these molecules are stacked to form columns that are close-packed. The distribution of diffuse scattering over the reciprocal plane perpendicular to the stacking direction indicates disorder between the stacks of molecules. Little information concerning the identity of ligands attached to the metal core could be discerned, but existence of the nine-membered ring with indication of an ordered Ni position could be substantiated from the analysis of the Bragg intensities. The equivalent $\{Cr_8Co\}$ wheel compound was synthesized; it showed very similar cell constants and intensity distribution but had even more pronounced diffuse scattering, and full structural characterization remained elusive.

In an attempt to improve the knowledge of the nona-nuclear wheel structure we decided to investigate a system in which the metal sites are more likely to be ordered. Whereas in **1** the nickel site is disordered over the eight metal positions, if vanadyl is used the octanuclear wheel that results, $[Et_2NH_2]$

[*] Dr. O. Cador, Prof. D. Gatteschi, Prof. R. Sessoli
Laboratorio di Magnetismo Molecolare
Dipartimento di Chimica & INSTM
Università degli Studi di Firenze
Polo Scientifico Universitario
Via Lastruccia n. 3, 50019 Sesto Fiorentino (Italy)
Fax: (+39) 055-4573372
E-mail: roberta.sessoli@unifi.it
Dr. G. A. Timco, Prof. R. E. P. Winpenny
Department of Chemistry
The University of Manchester
Oxford Road, Manchester, M13 9PL (UK)
Fax: (+44) 161-275-4616
E-mail: grigire.timco@man.ac.uk
richard.winpenny@man.ac.uk
Prof. F. K. Larsen, Dr. J. Overgaard
Department of Chemistry
University of Aarhus
Aarhus (Denmark)
Dr. A.-L. Barra
Laboratoire des Champs Magnetiques Intenses-CNRS
38042 Grenoble Cedex 9 (France)
Dr. S. J. Teat
CCLRC Daresbury Laboratory
Warrington, Cheshire, WA4 4AD (UK)

[**] This work was supported by the EPSRC(UK), the EC-TMR Networks "MolNanoMag" (HPRN-CT-1999-00012) and "QuEMolNa" (MRTN-CT-2003-504880), the German DFG (SPP 1137) and INTAS (00-00172).

  DOI: 10.1002/ange.200460211

$[Cr_6(VO)_2F_8(O_2CCMe_3)_{15}]$ **3**, has ordered metal sites, with the two VO^{2+} units next to each other within the wheel.[12] Therefore we treated chromium trifluoride with pivalic acid and dicyclohexylamine in the presence of vanadyl acetate. The product that formed was isolated as $[(C_6H_{11})_2NH_2][Cr_7(VO)_2F_9(O_2CCMe_3)_{17}]$ **4** (Figure 1). X-ray characterization demonstrates,[10] beyond doubt, that we have made nonanuclear metal wheels. Each Cr···Cr and Cr···V edge is bridged by one fluoride and two pivalate ions while the V···V edge is bridged by one fluoride ion and one pivalate ion.

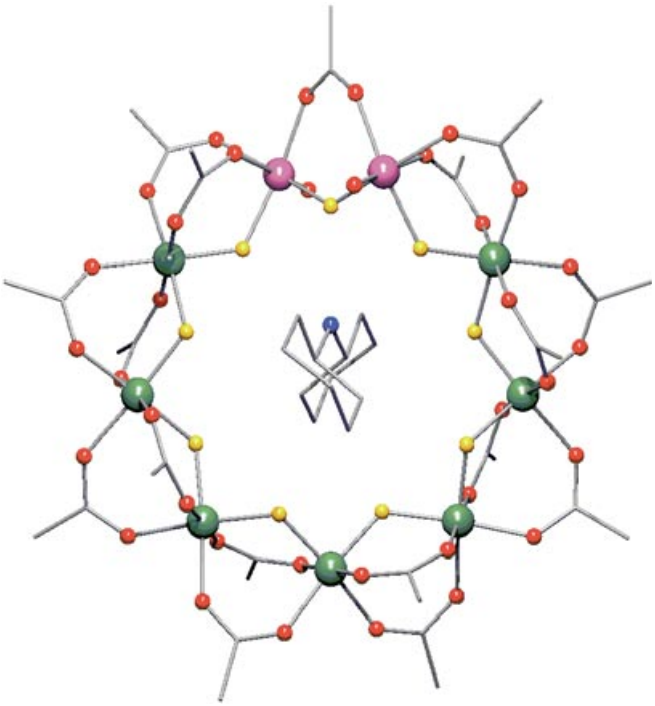

Figure 1. The structure of **4** in the crystal. The hydrogen atoms have been omitted for clarity. Bond length ranges [Å]: Cr–F 1.9098–1.9338, Cr–O 1.915–1.968, V–F 1.9494–2.0114, V–O(oxide) 1.580, V–O(pivalate) 1.989–2.185 (av esd 0.002). Cr dark green; V purple; F yellow; O red; N blue; C grey.

The magnetic behavior of these nonanuclear wheels is fascinating. Compound **2** contains an even number of unpaired electrons due to the presence of a Ni^{II} ion, with $S=1$, and eight Cr^{III} ions with $S=3/2$ spins; this allows a diamagnetic ground state, and therefore **2** is not a typical example of a frustrated system: for example, the doubly degenerate $S=1/2$ ground states predicted to occur in odd-membered rings of half-integer spins. Nevertheless in **2** not all the antiferromagnetic interactions can be simultaneously satisfied and therefore it can be regarded as frustrated.[13] A way to visualize the problem is its analogy with the Möbius strip, which better reflects the finite size of this system, compared to standard soliton or domain-wall pictures. The odd number of spins makes it impossible for all spins to align antiparallel to their nearest neighbor—as preferred where the exchange is antiferromagnetic. We can think of the region where the neighboring spins are alternately "up and down" as the flat region of the Möbius strip, while a "knot" occurs between the nearest neighbors where the spins cannot be arranged antiparallel. More interesting and much less obvious is how the presence of this knot in the ring manifests itself in the magnetic properties.

The temperature dependence of the magnetic molar susceptibility, χ_M, is shown in Figure 2. At room temperature

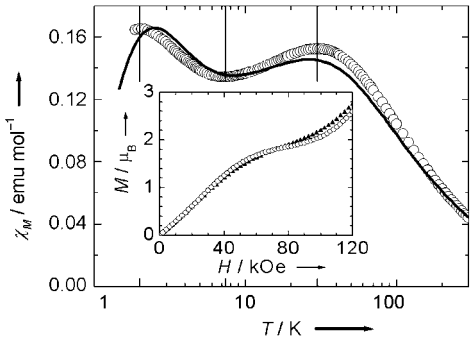

Figure 2. Variation of χ_M with temperature for **2.** The solid line corresponds to the calculated values with $J=16$ K, $J'=70$ K, and $\langle g\rangle=2$. In the inset the magnetization versus field measured at 1.6 K (○) and 2.0 K (▲) is shown.

the $\chi_M T$ value is equal to 13.2 emu K mol^{-1}, lower than expected (16 emu K mol^{-1}) for eight Cr^{III} and one Ni^{II} isolated spins with $g=2.00$. This may indicate that strong antiferromagnetic interactions are already operative at room temperature. χ_M increases when the temperature is lowered down to $T_{max1}=30$ K, at which it passes through a broad maximum, and then decreases when the temperature is lowered further. At $T_{min}=7.4$ K it passes through a minimum then increases again, and finally reaches a second maximum at $T_{max2}=2$ K. This behavior is unusual and to our knowledge has never been observed before. What is common, and expected, is the presence of one maximum in a χ_M vs. T curve as observed for antiferromagnetic homometallic even-membered wheels, for example, **1**.

The magnetic properties of the system are determined by Heisenberg-type superexchange interactions between the magnetic centers. The simplest Hamiltonian describing the system is the following:

$$\mathscr{H} = J'(\boldsymbol{S}_{Cr_1}\boldsymbol{S}_{Ni} + \boldsymbol{S}_{Cr_8}\boldsymbol{S}_{Ni}) + J\sum_{i=1}^{7}\boldsymbol{S}_{Cr_i}\boldsymbol{S}_{Cr_{i+1}} \quad (1)$$

in which J' and J are the superexchange coupling parameters between the nickel spin and its two chromium neighbors and between the nearest neighbor chromium ions, respectively. The $\boldsymbol{S}_i$ values are the spin quantum operators associated with spin values $S_{Ni}=1$ and $S_{Cr}=3/2$ of nickel and chromium ions, respectively. The presence of two maxima strongly indicates an $S=0$ ground state. The first step was to simulate the χ_M versus T curves for several sets of parameters J and J'. Based on previous work on Cr_8 wheels, we set J/k_B to 16 K. J'/k_B was varied between zero and 70 K. Only when $J'/k_B > 36$ K are two maxima in the susceptibility observed (Figure 3).

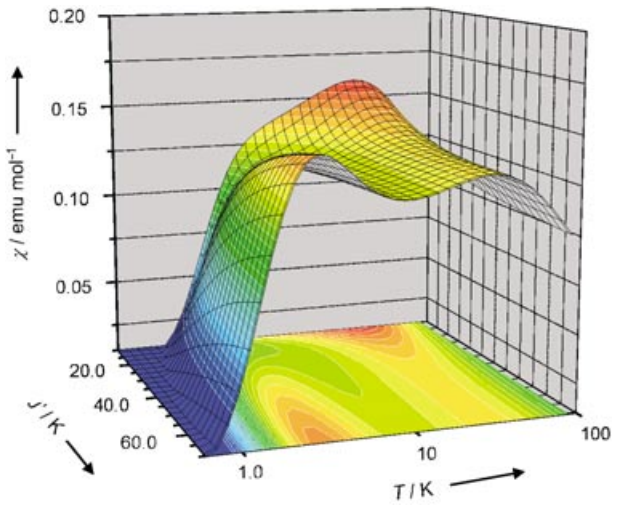

Figure 3. Simulation of the variation of χ_M as a function of both T (log scale) and J'. J has been set equal to 16 K.

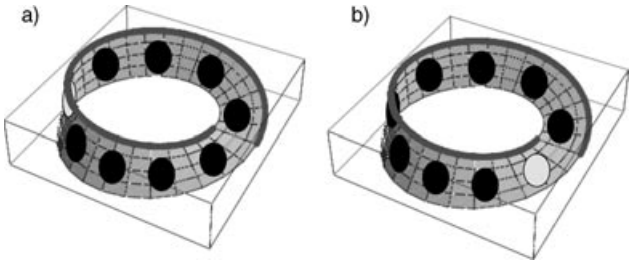

Figure 4. Representation of the spin frustration in **2** as a Möbius strip, with the white circle as the Ni site, and black circles as Cr. The knot is the point at which the thick grey line is discontinuous: a) with $J' \gg J$ and the knot on the chromium chain; b) with $J' < J$ and the knot is at nickel.

Qualitatively the observation of two maxima in the χ versus T curve can be explained by the presence of several states with low total spin values (S_T) that are very close in energy to the ground $S_T = 0$ state. If $J' = 0$ the ground state is $S_T = 1$ because the spin of the nickel is not correlated to the antiferromagnetic chain of chromic spins. Inclusion of an antiferromagnetic J' rapidly stabilizes a diamagnetic ground state, with the first three excited states being characterized by $S_T = 1$. A ferromagnetic J', even if does not remove spin frustration, stabilizes an $S = 2$ ground state with disappearance of the maxima in the χ versus T curve. An antiferromagnetic Cr^{III}–Ni^{II} interaction has been unambiguously observed in a similar $\{Cr_7Ni\}$ ring.[9]

To discuss the "knot" of the Möbius strip, that is, the point at which the spins on nearest neighbors are not antiparallel, the eigen vectors of the low lying states are needed. In this particular case it is very convenient to use for the basis set the representation in which we couple the chromic spins on odd sites to give an intermediate spin S_{odd} and analogously for the spins on the even sites, S_{even}. These two intermediate spins are coupled together, to give the total spin for the chromium chain, S_{TCr}, and this last is coupled to the spin of the nickel to give the total spin, S_T. There are 2764 different ways of obtaining an $S_T = 1$ state, therefore the wave functions of Hamiltonian (1), are linear combinations $\psi = \sum_{i=1}^{2764} c_i \varphi_i$. However, for the states lowest in energy only few c_i's are significantly different from zero. The composition of the first excited $S_T = 1$ state strongly depend on the J'/J ratio. If $J' < J$ ψ_1 is mainly given by $S_{even} = 6$, $S_{odd} = 6$, with $S_{TCr} = 0$ and can be seen as mainly given by the uncorrelated spin of the nickel ion. The knot is then localized on the nickel site, as shown in Figure 4b. On the contrary when $J' \gg J$ the largest contribution comes from $S_{TCr} = 2$ antiferromagnetically coupled with the nickel spin to give $S_T = 1$. In this case the "up–down" orientation of spins is more rigid at the nickel site and the knot is instead delocalized on the chromium chain as shown in Figure 4a.

A measurement of the magnetization does not usually provide information on the wave function composition and more sophisticated techniques must be used. As Ni^{II} and Cr^{III} ions have significantly different g values, 2.2 versus 1.98, respectively, an accurate measurement of the g values of the lowest excited state will directly reflect the composition of the wave function. By using the spin projection techniques it is relatively easy to calculate the g factor of the different φ_i states starting from the values of the single ions. For the $S_{TCr} = 0$ $S_T = 1>$ state $g = g_{Ni} = 2.2$, whereas for $S_{TCr} = 2$ $S_T = 1 > g = {}^3/_2 g_{Cr} - {}^1/_2 g_{Ni} = 1.86$. In intermediate cases the calculation of g requires us to consider the contribution of all φ_i states which appear in ψ_1 with a $c_i \neq 0$. The same procedure can be applied to any state ψ.

A true fitting procedure of the χ versus T curve is hampered by the strong g dependence on the spin state that has a stronger effect on the value of χ than J'. To take into account the wavefunction composition of the excited states is an unmanageable task, given the dimension of the S subspaces in the spin Hamiltonian matrix. In Figure 2 we report the χ versus T curve calculated for $J = 16$ K and $J' = 70$ K. The spectrum of low-lying energy states shows the first and second $S = 1$ states at ≈ 3.7 and ≈ 10.7 K from the $S = 0$ ground state, respectively. The first $S = 2$ is calculated to occur at ≈ 22 K above the ground state. This energy scheme is not significantly varied if J' is reduced by a factor of two, as is usual in the presence of spin frustration. The M versus H curve shows a first plateau at about 1.8 μ_B ,which is in agreement with the predicted $g < 2$ value. Interestingly a maximum in the dM/dH curve at 1.6 K is observed around 28 kOe (not shown). This observation suggests a gap between the ground and the first excited $S = 1$ state of about 3 K, which is in agreement with the calculated energy spectrum. The further increase of M above 100 kOe, without reaching the plateau at about 4 μ_B expected for an $S = 2$ state, suggests that the first $S = 2$ state starts to be populated at these fields, but that it is at least 15 K above the first $S = 1$ state, as calculated.

To confirm our interpretation, we have used electron paramagnetic resonance (EPR) spectroscopy. In Figure 5 we report the polycrystalline powder high field EPR spectra recorded at a frequency of 285 GHz; an unconventionally high frequency has been used to better resolve the difference in the g value. At 20 K a single isotropic line is observed centered at $g \approx 2$, as a result of many populated spin states. On

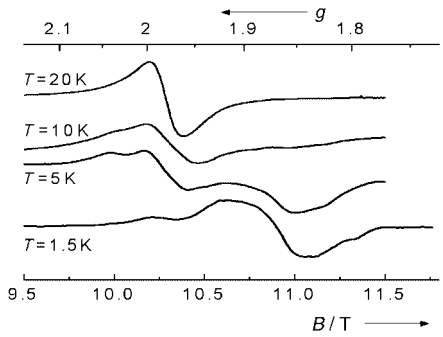

Figure 5. Variable-temperature EPR spectra of **2** recorded at 285 GHz by using a laboratory built spectrometer based on a Gunn diode source of far-infrared radiation.

lowering the temperature, a line centered at $g = 1.86$ increases in intensity at the expense of the line at $g \approx 2$, confirming that the lowest magnetic state has a g factor significantly smaller than 2. Similar results are obtained at 190 GHz. The lines have a nonresolved fine structure, probably due to the magnetic anisotropy (the so called zero-field splitting) of the states, but the observed shift to low g values on lowering the temperature unambiguously confirms that $J' \gg J$ as suggested also by the presence of two maxima in the magnetic susceptibility. The spin frustration is therefore delocalized on the chromium chain, as represented by the Möbius strip of Figure 4a.

This heterometallic odd-membered ring provides a fascinating example of how the supramolecular approach can be used to observe new magnetic phenomena. It possible to tune the delocalization of the frustrated bonds in the ring and to detect it in a very simple way, thus providing a text book example of spin frustration. Similar phenomena are observed in **4** and detailed studies will be reported later.

Experimental Section

2: $CrF_3 \cdot 4H_2O$ (5.0 g, 28 mmol), $(cy\text{-}C_6H_{11})_2NH$ (2.1 g, 12 mmol), basic nickel carbonate ($2NiCO_3 \cdot 3Ni(OH)_2 \cdot 4H_2O$; 0.5 g, 0.9 mmol) and Me_3CCO_2H (15.0 g, 147 mmol) were heated at 140 °C for 7.0 h, then allowed to cool to room temperature. Acetone (50 mL) was added and the resulting mixture was stirred for 15 mins. The microcrystalline product was filtered, washed with a large quantity of acetone, dried in air, dissolved in hot THF (75 mL), filtered, and the filtrate was diluted with toluene (40 mL). The solution was concentrated by evaporation at approx. 40 °C to 30 mL and then very slowly cooled to room temperature. The solution was left to stand for 24 h to yield green hexagonal crystals, which were isolated by filtration and washed with toluene; yield 1.7 g (17 %, calculated from $CrF_3 \cdot 4H_2O$). Elemental analysis calcd(%) for $C_{116}H_{202}Cr_8F_9NNiO_{36}$: Cr 14.69, Ni 2.07, C 49.19, H 7.19, N 0.49, F 6.04; found: Cr 14.51, Ni 1.83, C 49.64, H 7.25, N 0.48, F 5.85. ESMS m/z (%): −2465 (100) $[Cr_8NiF_9(O_2CCMe_3)_{18}]^-$; +2671 (100) $[M+Na]^+$; +2511 (50) $\{[Cr_8NiF_9(O_2CCMe_3)_{18}]+2Na\}^+$.

4: $CrF_3 \cdot 4H_2O$ (5.0 g, 28 mmol), $(C_6H_{11})_2NH$ (2.40 g, 13.2 mmol) and Me_3CCO_2H (14.0 g, 137 mmol) were heated with stirring at 140 °C for 2.0 h. $[VO(O_2CCMe_3)_2]_n$[14] (1.5 g, 5.6 mmol when $n = 1$) was added, and the mixture then heated for 4.0 h. The reaction mixture was cooled to room temperature, acetone (30 mL) was added, and the solution was stirred for a further 15 mins. A green solid was collected by filtration, washed with acetone (3 × 15 mL) and dried in air. The product was separated by column chromatography on silica gel by using toluene as eluent. It was eluted as the first band from the column. The solution was then evaporated to dryness under reduced pressure and the residue was redissolved in warm hexane (150 mL). Slow evaporation of the solvent at ambient temperature produced X-ray quality green crystals of **4** after two weeks. Crystals were collected by filtration washed with cold hexane and dried on air at room temperature; yield 2.15 g (30 %; calculated from $[VO(O_2CCMe_3)_2]_n$). Elemental analysis calcd (%) for $C_{97}H_{177}Cr_7F_9N_1O_{36}V_2$: Cr 14.16, V 3.96, C 45.33, H 6.94, N 0.54, F 6.65; found: Cr 14.08, V 4.10, C 45.49, H 6.62, N 0.48. F 6.37. ESMS m/z (%): −2387 (100 %) $[Cr_7(VO)_2F_9(O_2CCMe_3)_{17}]^-$.

Magnetic measurements: magnetic measurements were recorded on a polycrystalline powder samples with an Oxford Instruments Vibrating Sample Magnetometer (VSM) operating in the temperature range 1.5–300 K with magnetic fields up to 120 kOe. It has been checked that the magnetic susceptibility was independent of the amplitude of the applied field by recording the magnetization with two different magnetic fields, 1 and 10 kOe.

Received: April 2, 2004
Revised: July 8, 2004

Keywords: cage compounds · chromium · heterometallic complexes · magnetic properties · spin frustration

[1] K. L. Taft, C. D. Delfs, G. C. Papaefthymiou, S. Foner, D. Gatteschi, S. J. Lippard, *J. Am. Chem. Soc.* **1994**, *116*, 823–832.
[2] R. E. P. Winpenny, *Comprehensive Coordination Chemistry II, Vol. 7* (J. A. McCleverty, T. J. Thomas), Elsevier, Oxford, **2004**, pp. 125–176, and references therein.
[3] a) B. Hasenknopf, J.-M. Lehn, B. O. Kneisel, G. Baum, D. Fenske, *Angew. Chem.* **1996**, *108*, 1987–1990; *Angew. Chem. Int. Ed. Engl.* **1996**, *35*, 1838; b) C. S. Campos-Fernádez, R. Clérac, J. M. Koomen, D. H. Russell, K. R. Dunbar, *J. Am. Chem. Soc.* **2001**, *123*, 773–774.
[4] G. Mezei, P. Baran, R. G. Raptis, *Angew. Chem.* **2004**, *116*, 584–587; *Angew. Chem. Int. Ed.* **2004**, *43*, 574–577.
[5] V. L. Pecoraro, A. J. Stemmler, B. R. Gibney, J. J. Bodwin, H. Wang, J. W. Kampf, A. Barwinski, *Prog. Inorg. Chem.* **1997**, *45*, 83–117.
[6] G. Toulouse, G. *Comm. Phys.* **1977**, *2*, 115–119.
[7] F. Nori, E. Gagliano, S. Bacci, S. *Phys. Rev. Lett.* **1992**, *68*, 240–243.
[8] V. Caignaert, E. Suard, A. Maignan, Ch. Simon, B. Raveau, *J. Magn. Magn. Mater.* **1996**, *153*, L260–L264.
[9] F. K. Larsen, E. J. L. McInnes, J. Overgaard, S. Piligkos, G. Rajaraman, E. Rentschler, A. A. Smith, G. M. Smith, G. A. Timco, R. E. P. Winpenny, *Angew. Chem.* **2003**, *115*, 105–109; *Angew. Chem. Int. Ed.* **2003**, *42*, 101–105.
[10] Crystal data for **2**: ($C_{102}H_{186}Cr_8F_9NNiO_{36}$; $M_r = 2648.41\ g\,mol^{-1}$): dark green hexangular shaped blocks, orthorhombic, space group possibly *Pbna*, $a = 19.587(5)$, $b = 24.818(6)$, $c = 33.925(9)$ Å, $V = 16490(7)$ Å^3, $Z = 4$, $T = 200(2)$ K, $\rho = 1.067\ g\,cm^{-3}$, $F(000) = 5576$, $\mu(MoK_\alpha) = 0.683\ mm^{-1}$. Crystal data for **4** $C_{101.5}H_{187.5}Cr_7F_9NO_{36}V_2$: $M_r = 2634.9\ g\,mol^{-1}$; green prism, orthorhombic, space group *Pbcn*, $a = 23.9765(13)$, $b = 31.2265(18)$, $c = 19.3562(11)$ Å, $V = 14492(1)$ Å^3, $Z = 4$, $T = 150(2)$ K, $\rho = 1.208\ g\,cm^{-3}$, $F(000) = 5546$, $\mu(Mo_{K\alpha}) = 0.701\ mm^{-1}$.Data were collected on Bruker SMART CCD diffractometers ($Mo_{K\alpha}$, $\lambda = 0.71069$ Å for **2** and 0.6898 Å for **4**). Selected crystals were mounted on the tip of a glass pin by using Paratone-N oil and placed in the cold flow produced with an Oxford Cryocooling device. Complete hemispheres of data were collected using ω-scans (steps of 0.6° for **2** and 0.3° for **4**, 30 s frame^{-1}). Integrated intensities were obtained with

SAINT+[11] and they were corrected for absorption by using SADABS.[11] Structure solution and refinement was performed with the SHELX program.[11] The structures were solved by direct methods and **3** was completed by iterative cycles of ΔF syntheses and full-matrix least-squares refinement against F^2 to give, for **4** by using 705 parameters and 418 restraints, $wR_2 = 0.2241$ (19676 unique reflections), $R_1 = 0.0681$ (14946 reflections with $I > 2\sigma(I)$). For **2** the structure did not develop past the localization of the atomic structure of the nona-metallic wheel and the octahedral first coordination sphere of the metals. CCDC-231873 (**4**) contains the supplementary crystallographic data for this paper. These data can be obtained free of charge via www.ccdc.cam.ac.uk/conts/retrieving.html (or from the Cambridge Crystallographic Data Centre, 12 Union Road, Cambridge CB21EZ, UK; fax: (+44) 1223-336-033; or deposit@ccdc.cam.ac.uk).

[11] G. M. Sheldrick, Programs for Crystal Structure Analysis, University of Göttingen, **1998**.

[12] F. K. Larsen, J. Overgaard, S. Parsons, E. Rentschler, G. A. Timco, A. A. Smith and R. E. P. Winpenny, *Angew. Chem.* **2003**, *115*, 6160 – 6163; *Angew. Chem. Int. Ed.* **2003**, *42*, 5978 – 5981.

[13] O. Kahn, *Chem. Phys. Lett.* **1997**, *265*, 109 – 114.

[14] R. C. Paul, A. Rumar, *J. Inorg. Nucl. Chem.* **1965**, *27*, 2537 – 2547.

